Remote Sensing of Environment 236 (2020) 111500

Contents lists available at ScienceDirect

Remote Sensing of Environment

journal homepage: www.elsevier.com/locate/rse

Arctic rock coast responses under a changing climate

Michael Lim[a,*], Mateusz C. Strzelecki[b,f], Marek Kasprzak[b], Zuzanna M. Swirad[c], Clare Webster[d], John Woodward[a], Herdis Gjelten[e]

[a] Engineering and Environment, Ellison Building, Northumbria University, Newcastle Upon Tyne, NE1 8ST, UK
[b] Institute of Geography and Regional Development, University of Wrocław, pl. Uniwersytecki 1, 50-137, Wroclaw, Poland
[c] Department of Geography, Durham University, South Road, DH1 3LE, Durham, UK
[d] WSL Institute for Snow and Avalanche Research SLF, Davos, Switzerland
[e] Observation and Climate Department, Norwegian Meteorological Institute, PO Box 43 Blindern, NO-0313, Oslo, Norway
[f] Alfred Wegener Institute, Helmholtz Centre for Polar and Marine Research, Permafrost Research, 14473, Potsdam, Germany

ARTICLE INFO

Keywords:
Structure from motion
Photogrammetry
Terrestial laser scanning
Arctic geomorphology
Climate change
Rock coasts
Temperature mapping

ABSTRACT

It has been widely reported that Arctic sea ice has decreased in both extent and thickness, coupled with steadily rising mean annual temperatures. These trends have been particularly severe along the rock coast of southern Svalbard. Concerns have been raised over the potential for higher energy storms and longer ice-free open water seasons to increase the exposure of Arctic coasts, and consequently the concentration of infrastructure critical to Arctic community survival, to enhanced rates of erosion. Here we present and apply innovative remote sensing, monitoring and process analyses to assess the impact of recent coastal climatic changes. High resolution analyses demonstrate that the small scale ($< 0.001\ m^3$) changes that are rarely considered quantitatively exhibit geomorphic responses distinct from those of larger, more readily detected cliff failures. We monitor temperature depth profiles in both the shore platform and the cliff face to show rock sensitivity over time to both global and local influences. The results demonstrate the efficacy of thermal processes on Arctic rock cliffs relative to platforms, and may hold implications for understanding strandflat development rates. New three-dimensional thermography (thermal mapping) and process zone characterisation has been used to spatially assess the sensitivity of Arctic rock coast responses to contemporary processes on deglaciating coasts. Through the spatial and temporal analyses of key geomorphic behaviour zones and comparison over a range of sites, the complex and changing interplay between subaerial weathering and cryogenic and intertidal processes has been highlighted. These data challenge long standing assumptions over the future of Arctic rock coasts and identify new, focused lines of enquiry on the decline in cryogenic processes and understanding the sensitivity of Arctic rock coasts to climatic changes.

1. The dynamics of Arctic rock cliff systems

High latitude coastal rock environments provide vital access points to Arctic communities, resources and transport routes (Forbes, 2011). Many of the world's critical oil and gas pipelines pass through polar rock coast environments and the continued exploitation of petroleum reserves in the Arctic is likely to increase operations in and dependency upon them. Over a third of Arctic coastlines are rock dominated (Strzelecki, 2017) but the roles and significance of cryospheric influences such as permafrost, sea ice, icebergs, ice floes and ice-foot development relative to other coastal processes in determining the rate and nature of change remains contentious and potentially subject to regional variations (Hansom et al., 2014; Trenhaile, 1997). Coastal rock cliffs in Arctic environments typically experience strong seasonal variations from ice covered winters, through spring melt, thaw and sea-ice break-up to more typical marine conditions during summer; and as such they are potentially important geoindicators of changes to these controls (Forbes and Taylor, 1994). It has been suggested that the reduction of sea-ice in many cold regions has led to more exposed coastal conditions and intensified erosional processes (Forbes, 2011; Forbes and Taylor, 1994; Overeem et al., 2011; Strzelecki, 2011). However, rock coasts are often inaccessible and hazardous, with perceptibly slow and episodic rates of change making the significance and contribution of erosional processes difficult to quantify (Berthling and Etzelmuller, 2011). Rock coast science is significantly under-represented within coastal research relative to their extensive and dominant global

* Corresponding author.
E-mail address: michael.lim@northumbria.ac.uk (M. Lim).

https://doi.org/10.1016/j.rse.2019.111500
Received 23 June 2019; Received in revised form 18 October 2019; Accepted 26 October 2019

distribution (up to 70% of the world's coastlines, Naylor et al., 2010), and there is a particular paucity of data on polar systems (Byrne and Dionne, 2002; Hansom et al., 2014; Hinzman et al., 2005; Overduin et al., 2014; Trenhaile, 1997).

The few studies undertaken on polar rock slopes typically rely on relatively short-term (exceptionally up to five years) laboratory simulations (Hall, 1988), monitoring of flaking from control surfaces (up to 1 m^2) or the collection of debris at the foot of the cliff (Matsuoka et al., 1996). These approaches have enabled initial estimates of process rates from accessible rock walls, but provide little indication of the source location and spatial and temporal distribution of specific events; cliff foot debris is often subject to rapid fragmentation, scattering and removal. Attempts have been made to use photogrammetry to quantify Arctic cliff processes (Wangensteen et al., 2007), but have remained limited by the spatial coverage and, critically, the temporal extent of the data. Elsewhere changes in the rate and nature of cliff behaviour has been shown to be quantifiable through terrestrial laser scanning (TLS; Rosser et al., 2013), revealing insights into geomorphic responses and local conditioning of failure processes (Lim et al., 2011). More recently, structure from motion (SfM) photogrammetry from both airborne and ground based platforms has provided new three-dimensional detail on coastal rock slope environments (Westoby et al., 2018) and their geomorphic behaviour (Gilham et al., 2018). Short-term variability and episodic behaviour in rock slopes generally is thought to converge to a constant over longer timescales (Budetta et al., 2000) and it is the long-term rates of change that underpin how rock coasts are modelled and managed (Limber and Murray, 2011). Establishing the contribution of environmental changes to both the degradation and failure of rock cliffs remains problematic (Coombes, 2011; Lim et al., 2011). However, the extreme process conditions experienced in polar rock environments may hold greater potential to detect and analyse process-response relationships (see for example André, 1997; Matsuoka et al., 1996; Naylor et al., 2017; Rapp, 1957; Sass, 2005; Wangensteen et al., 2007).

An essential challenge for Arctic rock coast science is to obtain data of sufficient resolution to account for geomorphic behaviour and over scales great enough to assess process responses to climatic changes (Lantuit et al., 2012; Trenhaile, 1983). This paper analyses Arctic cliff process rates using modern high resolution remote sensing, geomorphic zone characterisation and change detection in order to help address long-standing questions regarding the response of polar coastal cliff processes to environmental drivers of change.

2. Regional setting

Arctic coastal rock cliffs (or rock walls) represent a key diagnostic link between marine conditions, periglacial and paraglacial processes and climatic variations (Prick, 2002). Of note within the High Arctic is Svalbard (a Norwegian archipelago in the Arctic Ocean; Fig. 1a), a region undergoing a distinct and sustained rise in mean annual temperatures (Gjelten et al., 2016) and thought to be of unique climate sensitivity (Etzelmüller et al., 2011).

An early suite of studies undertaken by Jahn (1961) focussed on quantifying the rates of change in high Arctic coastal rock cliffs, as part of a wider investigation into periglacial processes in Spitsbergen, the main island in the Svalbard archipelago. The primary site for this investigation (and that of Jahn, 1961) are the Veslebogen cliffs, located in Hornsund at the southern tip of Spitsbergen (Fig. 1a), where climatic changes have been particularly severe (Jakacki et al., 2017). Hornsund is located at the northern extreme of the warmer North Atlantic current before it enters the colder Arctic Ocean (Rasmussen et al., 2007). Mean annual temperatures (MAT) have been rising at a rate of 1–1.3 °C per decade since the late 1970's with distinct warmer and cooler periods overlain on a general rising trend (Gjelten et al., 2016). There has been a coincident decline in perennial sea-ice at a rate of 13.5% per decade (Parkinson and Comiso, 2013), which has resulted in greater exposure to storm events (Lantuit et al., 2012). The sensitivity of Hornsund to climatic variations is evident in long-term temperature reconstructions (Fig. 1c); the area typically experiences the mildest winters but the coolest summers in the region, perhaps reflective of sea-ice influence (Gjelten et al., 2016).

The cliffs at Veslebogen are approximately 8 m high and comprised of marble, with a series of spurs dividing small crenular embayments within the general form of the south facing cliffs (Swirad et al., 2017). Arctic tides are generally limited and the mean tidal range at Veslebogen is *c*. 1 m (Jakacki et al., 2017), with high tide just reaching the base of the cliff. The wider area has undergone coastal emergence through isostatic uplift and recent tectonics, with temporary periods of uplift reported to have accelerated average rates to 8.5 mm/yr since 2001 (Stemberk et al., 2015). The Hornsund fjord provides an effective filter on wave climate, generating relatively uniform wave conditions that reflect wind conditions (Herman et al., 2019). The prevailing easterly wind moderates incoming oceanic waves from the Greenland Sea although the coast is subjected to storm events. In winter snow drifts can accumulate at the base of the cliffs (Strzelecki et al., 2017), and in summer occasional rafts of icebergs collect on the southern and eastern orientated coastal sections, drifting westwards following calving events from the retreating Hansbreen (Fig. 1b).

In the late 1950's an ice-foot, a belt of ice formed from freezing seawater, ice floes and snow at the base of coastal cliffs (Nielsen, 1979), persisted nearly all year at the base of the Veslebogen cliffs (Jahn, 1961). This feature afforded a rare opportunity to gain accurate quantitative data on cliff processes through the collection and measurement of rock fall and abraded material accumulating on the ice-foot. By relating the volumes of failed material to the potential contributing source area, the rates of rock wall backwasting were calculated to be 0.03–0.05 m a^{-1} (Jahn, 1961). These rates from a significantly colder period (MAT in 1958 was −4.20 °C, in 2016 MAT was −0.02 °C) are a useful benchmark but, although the physical capture and analysis of easily identifiable rock fall material accumulating at the base of the cliff can be effective (Krautblatter et al., 2012), the true accuracy of these historic rates is hard to determine.

3. Data collection

3.1. Surface change detection

The ice-foot no longer persists until even early summer at the Veslebogen cliffs (it is largely absent by late May), preventing a direct repetition of Jahn's (1961) original approach. Instead, quantitative data on modern rates of change have been established through a series of high resolution remote sensing approaches. Repeat TLS and SfM photogrammetry have been used to generate digital elevation models (DEMs; 0.01 m resolution for cliff-wide surveys and 0.00001 m for close-range surface analyses) of the rock face at a range of scales. Surveys have been conducted during the summers of 2014; 2015; 2016 and 2017. A combination of TLS systems has been used: a Reigl VZ1000 with its longer range (up to 1 km) to set the context for the cliff changes, and a shorter range (up to 25 m) phase based Faro Focus3D to provide the detail. The exact method varied according to the availability of instruments but in general the Reigl scanner was deployed 20 m from the cliff face from 3 stations and the Faro at 10 m from the cliff face using 8 stations to account for the complex morphology, following recommendations for multiple viewpoint collections (Feagin et al., 2014). Data have been registered using RiScan Pro (v. 1.5.2) and the maximum alignment errors (root mean squared error; RMSE) for inter-survey registration and across different annual visits were 0.02 m and 0.03 m respectively. Data consistency has been assessed through the collection and differencing of two independent TLS datasets, collected in immediate succession (during the 2016 field season). Assuming no genuine changes had occurred (none were observed), occasional isolated patches of small (< 0.02 m) interpolated differences should also be considered in the application of error thresholds. Therefore, a

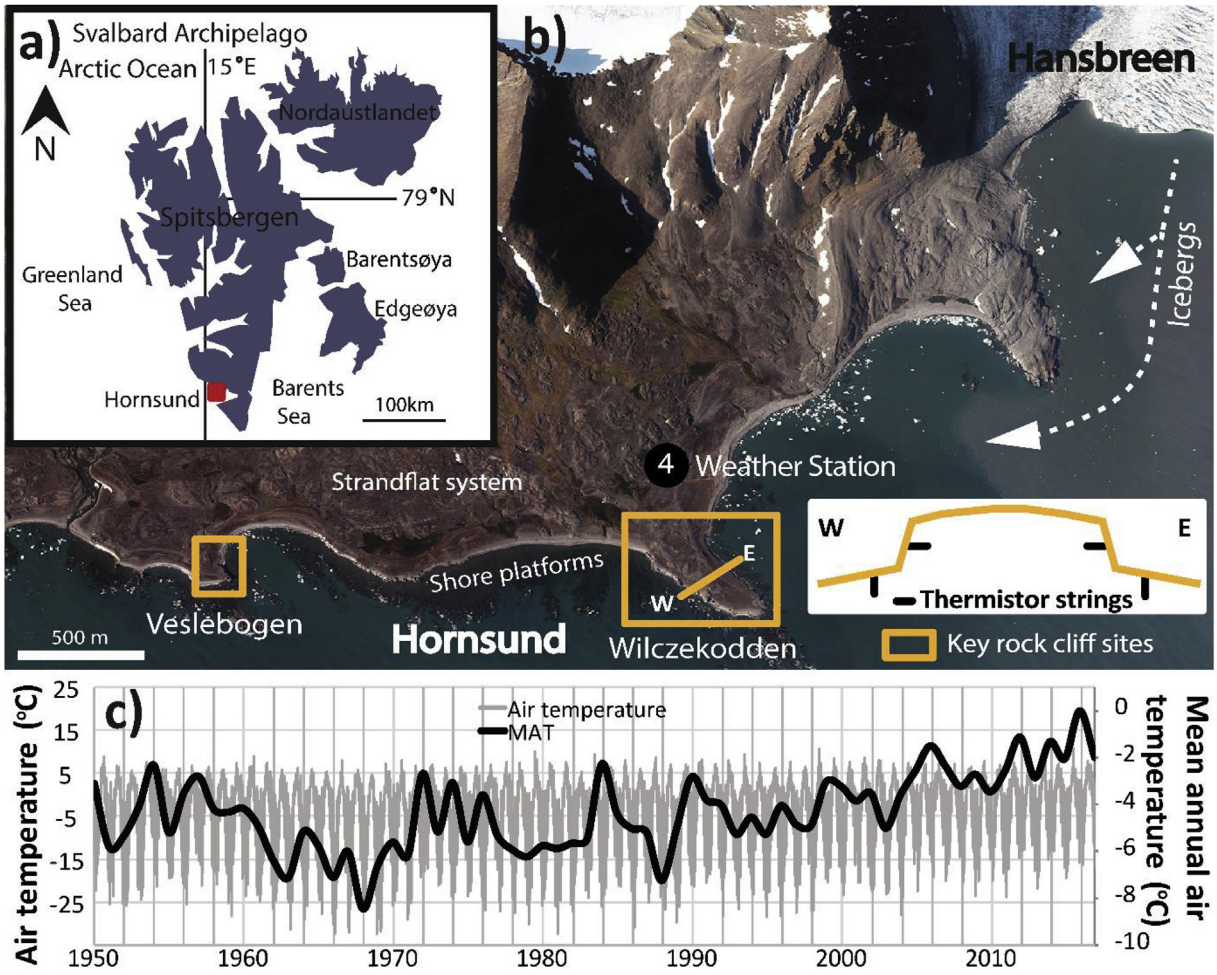

Fig. 1. (a), Regional setting of the main study area, (b), Local context of the main study area showing the influence of iceberg rafts from the retreating Hansbreen (a tidewater glacier) to the northeast and the positions of the thermistor strings (Fig. 4) and weather station used for the long-term air temperature series at Hornsund, southern Spitsbergen (c).

composite alignment and repeatability error threshold of 0.07 m has been applied to the change detection analyses.

Photogrammetry has been applied alongside the TLS in order to provide validation of the changes recorded, enabling reworked material at the cliff base to be excluded from the analysis. Multiple overlapping (> 90%) images have been collected with a 20 MP Sony RX10ii and processed in Agisoft PhotoScan (v. 1.2.4), utilising the guidelines suggested by Westoby et al. (2018), which optimise the survey distance by setting the range where the full cliff height fills the viewfinder and utilising sparse control concentrated towards the top and base of the cliff. The dense point clouds generated from the self-calibrating bundle adjustment have been refined by excluding points with a high (> 0.5 pixels) reprojection error or derived from too few (< 3) images. Manual point removal has been applied as a final editing stage to exclude unwanted or obviously erroneous areas. Check points have also been distributed over the surveyed area in a rough grid (constrained by the use of clearly identifiable natural features) and the errors detected were generally comparable to those of the TLS with a mean three-dimensional XYZ vector RMSE of < 0.04 m.

Thresholding, as applied to the data presented above, is a well-established approach to dealing with instrument and processing errors and uncertainties incurred in TLS applications (Lim et al., 2005; Rohmer and Dewez, 2015; Young et al., 2010). The application of SfM photogrammetry allows a high level of confidence to be achieved in the validity of the change data used but questions remain over the potential impact of the thresholding process itself on the distribution of changes produced. Thresholding is likely to produce conservative volumetric estimates of changes and to have a disproportionately large effect on the smallest changes that will be censored from the distribution. To further investigate the impact of thresholding on the change detection process, close range (< 0.5 m) SfM photogrammetry was applied specifically to gain quantitative data on the events occurring at scales below the detection threshold (1×10^{-3} m^3) established for the TLS surveys. A Sony RX10ii was used to capture the images and the collection strategy was adapted for close range by collecting images from a greater range of viewing angles to account for larger relative differences in perspective and occlusions, generally following a domed trajectory encompassing the area of interest. The photogrammetric results were first compared with traversing micro-erosion meter (TMEM) measurements on the flat shore platform, a high precision (sub-millimetre) point-based manual approach that is well established for monitoring coastal change related to rock surface lowering or swelling (Inkpen et al., 2010; Stephenson and Finlayson, 2009). The surface lowering rates derived from the two approaches were within 4×10^{-4} m a^{-1}, although a true point based comparison between the digital model (irregular point cloud data) and the physical pin measurements was hard to achieve with any certainly due to the precise nature of how the TMEM frame stabilised on the installed pins. The close range SfM approach was then applied to subsections (1 m^2) of the monitored cliff sections at each of the representative morphologies (namely within and above the intertidal zone on protruding spurs and inset bay back walls at three out of the six spur-bound bays) to revise the rate of occurrence

of low magnitude failures.

3.2. Thermal and geotechnical surface characterisation

In order to form a more complete and rigorous assessment of the rock material response to environmental processes, thermal photogrammetry has been developed to help characterise spatial variations across the monitored cliff section. Thermal images are used in building inspections to survey variations in material properties through, for example, the identification of areas of differential moisture content or thermal conductivity (Edis et al., 2014; Grinzato et al., 1998). In the natural environment, Luscombe et al. (2015) used thermal imaging to measure near surface hydrology. The tendency for each thermal image to be captured on an individually calculated maximum to minimum scale and the relatively low image resolutions achieved make quantitative analyses and feature matching in photogrammetric processing challenging. An Optris PI640 infrared camera (spectral range 7.5–13 μm) has been used to collect thermal images in the same manner as the colour based image collection described above (Section 3.1), optimising survey distance based on capturing the full height of the cliff and maximising image overlap.

All thermal images have been processed according to the approach described in Webster et al. (2018), although slight application specific variations require a brief summary here. The thermal images have been resampled to a single and consistent (minimum temperature 0 °C) colour-composite image (as opposed to the grayscale scalar used in Webster et al., 2018) range, resulting in images where each temperature had a unique colour identifier. The non-cliff areas have been masked and the standardised thermal images of the cliff processed photogrammetrically with Agisoft PhotoScan (v. 1.2.4). Clearly distinguishable thermal targets have been used to help scale and orientate the surface model that is subsequently converted back from a coloured point cloud to the original temperature scale as a three-dimensional thermal point cloud (Webster et al., 2018). The main aim of the thermal mapping has been to explore relative (rather than absolute) temperatures but point based temperature comparisons between thermal images and contactless infrared laser surface thermometer spot measurements were in close (generally < 1 °C) agreement for randomly selected points across all layers and a range of heights up the cliff. This variance is in line with the manufacturer's stated accuracy for the camera (± 2%).

The relative variations in temperature were compared with a vertical transect of Schmidt hammer (Proceq N-type Silver Schmidt) readings. The Schmidt hammer records the rebound force of a spring-loaded hammer in order to derive a non-destructive relative indication of rock strength. Readings are taken over a clean (outer algal and weathering crust removed with a grinding stone where necessary) rock surface in a grid pattern, producing an average hardness value from 25 measurements. After Strzelecki et al. (2017), hardness profiles at each site have been collected in vertical zones through the rock coast from the intertidal zone, through the high-water level, to the cliff toe and the cliff face to the cliff top.

4. Results

4.1. Arctic cliff recession

The cliffs had lower rates of retreat (Fig. 2) than were recorded for the same cliffs by Jahn (1961), although it is not currently possible to determine the validity of a quantitative comparison with physically derived historic rates. The highest annual modern cliff recession rate recorded was 0.019 m a^{-1}, which occurred between 2014 and 2015, a period when storm incidence was high and mean annual air temperature was cooler; −2.27 °C relative to −0.82 °C in 2015 - 16 and −1.55 °C in 2016–2017 (weather data provided by the Norwegian Meteorological Institute, after Gjelten et al., 2016; data calculated from summer to summer to reflect the survey schedule). The following year of monitoring (2015–2016) recorded an annual recession rate of 0.017 m a^{-1} and the final year of monitoring (2016–2017) produced a rate almost 50% lower than the first year (0.010 m a^{-1}). These modern rates are generally in line with the rates seen in coastal rock cliff environments in more temperate coastal settings (Kirk, 1977; Rosser et al., 2007; Sunamura, 1992). The spatial distribution of change during the highest monitored rates (2014–2015) was concentrated on areas protruding from the cliff face such as cliff tops, spurs and overhangs. These areas are potentially more exposed to high energy events, stress concentrations and mechanical action associated with snow, ice-foot and ice floe processes.

The distribution of failures has been further analysed through the relationship between the numbers of different sized failures that occurred from the rock cliffs (Fig. 2). The volume-frequency relationships for all years of monitoring follow power law distributions. The exponents are similar to rock fall distributions noted elsewhere (Guerin et al., 2014), and increase progressively from the first year, reflective of greater proportions of smaller events (or lower proportions of higher magnitudes) recorded within the size-frequency domain. Without continuous monitoring data it is not possible to correlate the occurrence of failures with specific triggers. However, the differences in spatial distributions of the failures recorded may reflect the relative quiescence in storm incidence and a reduction in the ice season following the 2014–2015 survey period, resulting in an increasing relative significance of smaller sized events. The length of the ice building season, defined by the number of frost days (simplified to temperatures < 0 °C), was 34 days longer during the first survey period (calculated from 1st July 2014 to 30th June 2015) than in the following two years (2015–2017, divided in the same manner). Frost days have been found to be the only significant climatic influence on retreat rate in a global analysis of rock coast erosion rates (Prémaillon et al., 2018), although direct causal relationships are complicated by lagged responses.

All annual rock fall distributions exhibit an inversion or roll-over at small magnitudes (< 0.001 m^3), but not at the highest magnitudes detected (up to 10 m^3). This under-representation of low magnitude changes in all survey data corresponds approximately to the minimum detection threshold applied to the data. Roll-over effects have been well documented in power-law distributions elsewhere (Barlow et al., 2012), but questions remain over whether they reflect genuine process effects or under-sampling resulting from the sensitivity of the change detection (van Veen et al., 2017).

Cullen et al. (2018) conducted a comprehensive analysis that demonstrated the ability of close-range SfM to detect sub-millimetre changes on rock surfaces of low relative topographic roughness. Many other studies have successfully employed TMEM data to assess surface downwearing processes (Strzelecki et al., 2017), but the spatial distribution and qualitative information gained from the SfM photogrammetry provide clear advantages to understanding micro-scale ($> 1 \times 10^{-6}$ m^3) surface change whilst maintaining a relatively close agreement with the TMEM dial gauge physical readings (Fig. 3; Cullen et al., 2018). In accordance with Cullen et al. (2018) we find relative topographic complexity a limitation on the accuracy of the high resolution, close range photogrammetric data. The embayment sub-sections had a slightly higher recession rate than the spurs (m^2 rates of surface lowering of 0.0006 m and 0.0004 m per yr respectively). When multiplied up to the scale of the whole cliff (accounting for the proportions of spurs and bays), rather than a roll-over below 1×10^{-3} m^3, high frequencies of low magnitude events appear to diverge from the original power law at scales below 1×10^{-6} m^3 (Fig. 3). The exact nature of the inflection, that appears to be scalable and relatively consistent across the several orders of magnitude detectable by the high resolution photogrammetric approach, remains undetermined, falling between the survey scales used. It is evident that spatial variability may play a key role in the low magnitude end of the size-frequency domain (also noted in Lim et al., 2010), placing greater emphasis on the

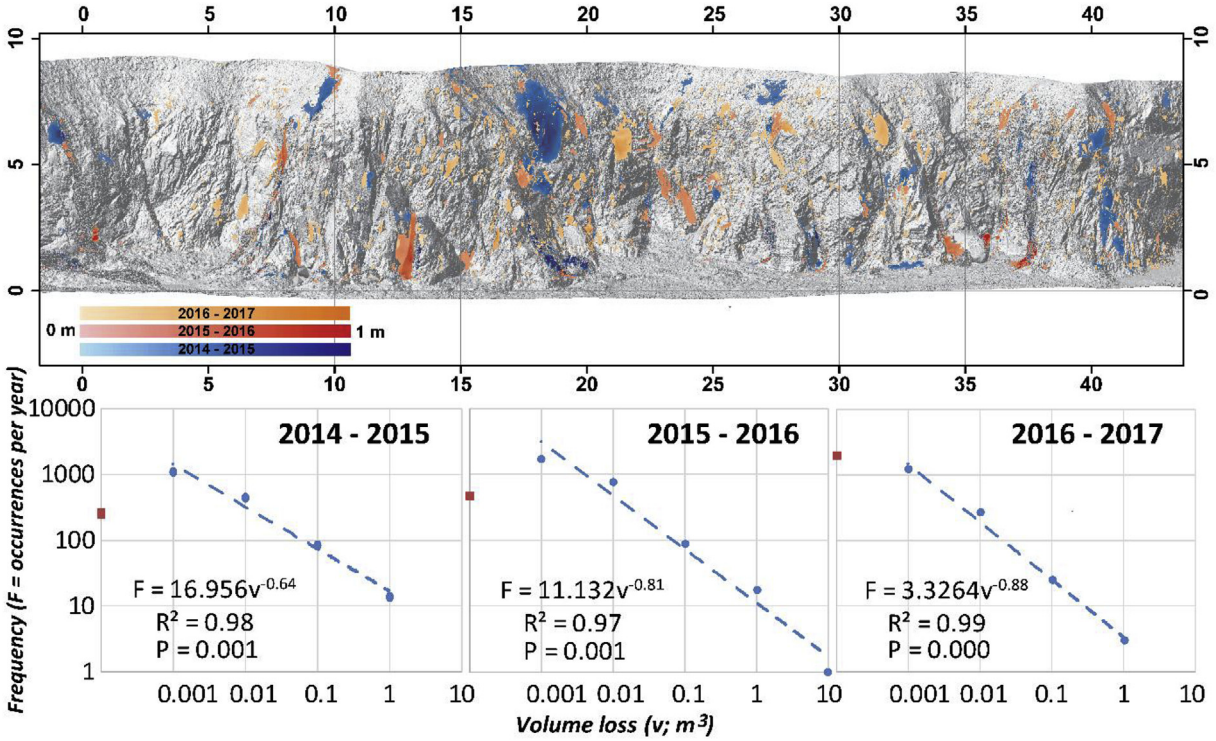

Fig. 2. Annual change map of the Arctic rock cliffs at Veslebogen overlain with a 5 m grid; SfM photogrammetry has been used to remove secondary surface changes associated with material reworking and beach level fluctuations. Magnitude-frequency diagrams below show a greater proportion smaller failures occurred during the 2015–2016 and 2016–2017 survey periods relative to that in 2014–2015 for the same monitored area. All three of the volume-frequency domains contain roll-over effects at lower magnitudes (denoted by the red squares). (For interpretation of the references to colour in this figure legend, the reader is referred to the Web version of this article.)

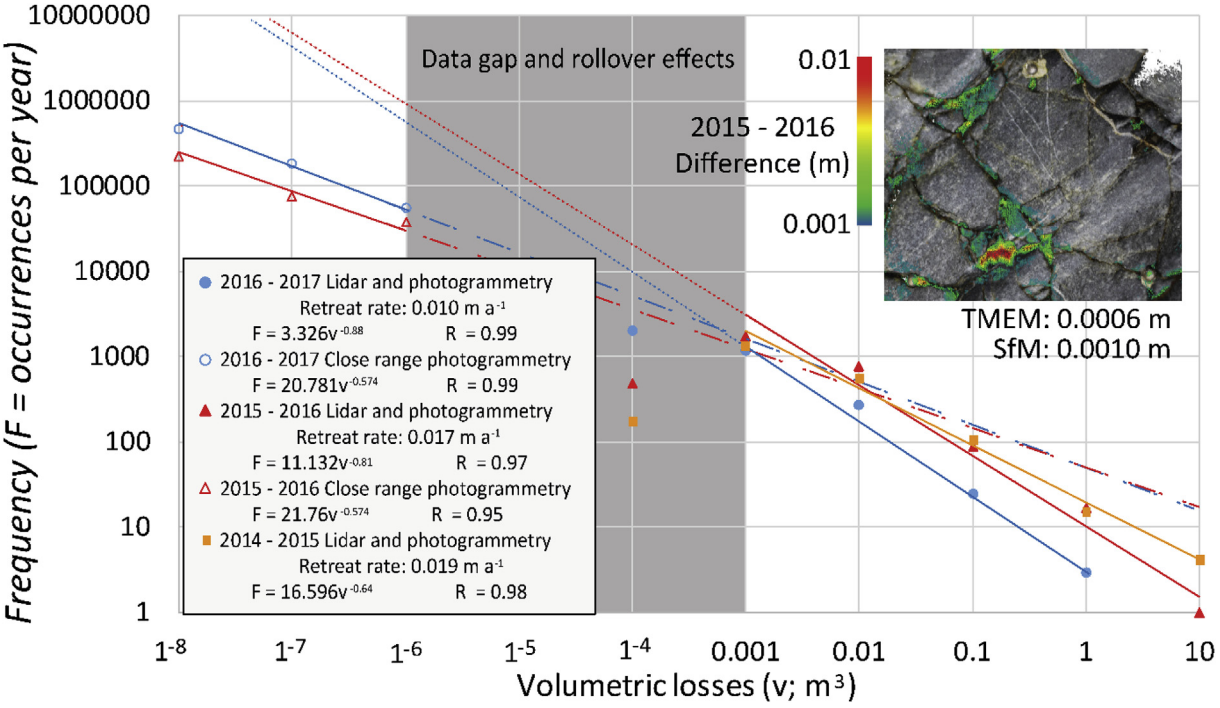

Fig. 3. Volumetric magnitude-frequency losses during three years of monitoring using TLS and photogrammetry for changes for monitored (solid lines) and modelled (dotted and dashed lines) magnitudes exceeding 1×10^{-3} m^3. From 2015 close range photogrammetry has been applied for changes below 1×10^{-6} m^3 (a minimum threshold of 1×10^{-8} has been imposed to reflect the inability to use TMEM validation on the rock wall). The image (top right) shows a SfM difference map (2015–2016) above a comparison between the average rate of surface lowering detected by TMEM and SfM on the shore platform to validate the approach. It should be noted that the TMEM detected swelling (positive elevation change), a common occurrence on shore platforms (Stephenson and Kirk, 2001), in multiple readings that reduced the averaged surface lowering result.

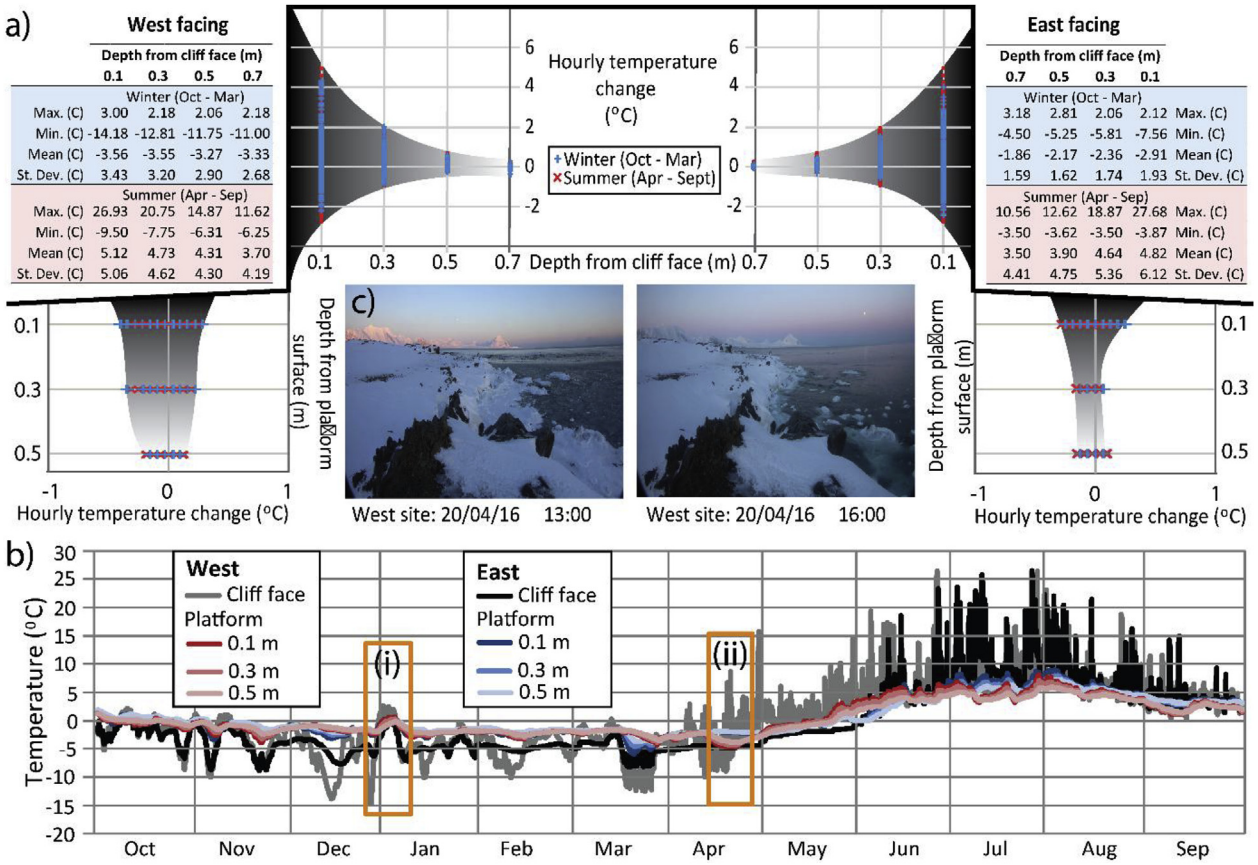

Fig. 4. Temperature change with depth in Arctic rock cliffs and platforms (a), Westerly and easterly aspects of the Wilczekodden peninsula (Fig. 1) are exposed to oceanic storm and iceberg influence respectively. Summary cliff face statistics are provided for both summer and winter periods (b), Rock temperatures through the year in shore platforms demonstrate a muted response relative to cliff face variations. Key thermal signatures highlighted (i and ii) represent an anomalous warming period and storm driven cooling event as break-up of the insulating ice-foot allowed cold water ingress over the platform (c), Before and after ice-foot break-up images.

identification of geomorphic process-responses spatially across the cliff.

4.2. Arctic rock coast geomorphic zones

Thermistor strings drilled into the cliff and platform either side of the Wilczekodden rock peninsula (Fig. 1b) demonstrate the interplay between cryogenic and marine influences. The moderating effects of coastal waters in summer and ice-foot in winter are evident in the muted rock platform thermal variations relative to those undergone by the cliff rock material (Fig. 4). The implication is that the efficacy of thermal stress effects (Collins and Stock, 2016) will be orders of magnitude greater horizontally into cliff material than vertically through platform material, forming a potential link between cryogenic temperature variations and strandflat enhancement. In early January 2016 there was a warming event related to an Atlantic wind storm designated 'Frank' by the U.K. Met Office that dragged warm moist air north into the Arctic (Kim et al., 2017). All rock to a depth of 0.5 m within both the cliff and platform recorded a distinguishable positive thermal response to these anomalous conditions (Fig. 4bi). The most pronounced warming was recorded in the west-facing cliffs (2 °C warmer than the east facing cliffs), which are more exposed to oceanic and storm influence. The influence of local setting controls is also evident in a rapid cooling event that occurred only in the western shore platform in late April (Fig. 4bii). Time-lapse imagery shows that this cooling was a result of storm driven break-up of the ice-foot, as cold water ingress reduced platform rock temperatures by several degrees within 3 h (Fig. 4c). The more sheltered east-facing cliffs were insulated by an ice-foot until late May. Subsequent short-term (several days) cooling effects from occasional iceberg rafts collecting on the east-facing coast have also been recorded from late May to early June and then less frequently throughout the summer. These influences of winter storm exposure and ice-foot dynamics on west-facing coasts and summer iceberg rafts from glacial discharge on the east-facing rock coast lead to highly responsive, locally conditioned seasonal thermal regimes (Fig. 4a).

Thermal links to rock fracture mechanics have been demonstrated as potential drivers of cyclic patterns of cumulative damage and ultimate failure (Collins and Stock, 2016). The penetration of thermal variance within the Arctic rock cliffs declines by over 60% below 0.1 m (to 0.3 m) on both the west and east coasts, a depth which also corresponds with the mean rock fall depth recorded during that period. We infer that thermal stress may provide a control on rock fall development and occurrence under Arctic conditions, similar to that established for exfoliation sheets (Collins and Stock, 2016), although other environmental factors such as bioprotection (Coombes et al., 2017) and humidity (Eppes and Keanini, 2017) may also condition the geomorphic response.

The three-dimensional temperature map of the Veslbogen cliffs revealed a general decrease in temperature from the base of the cliff upwards (Fig. 5). However, the temperature patterns were not even and in the sheltered embayments the weathered back walls demonstrated lower temperatures down to the cliff base, likely due to higher moisture content. The protruding areas displayed clearer zonation that appears to reflect the abrasive action at the cliff base transitioning up in layers and temperature increments to a 1.5 m thick capping layer of heavily weathered, compacted material above the rock mass.

The results of the rock hardness profiles show a quantitative

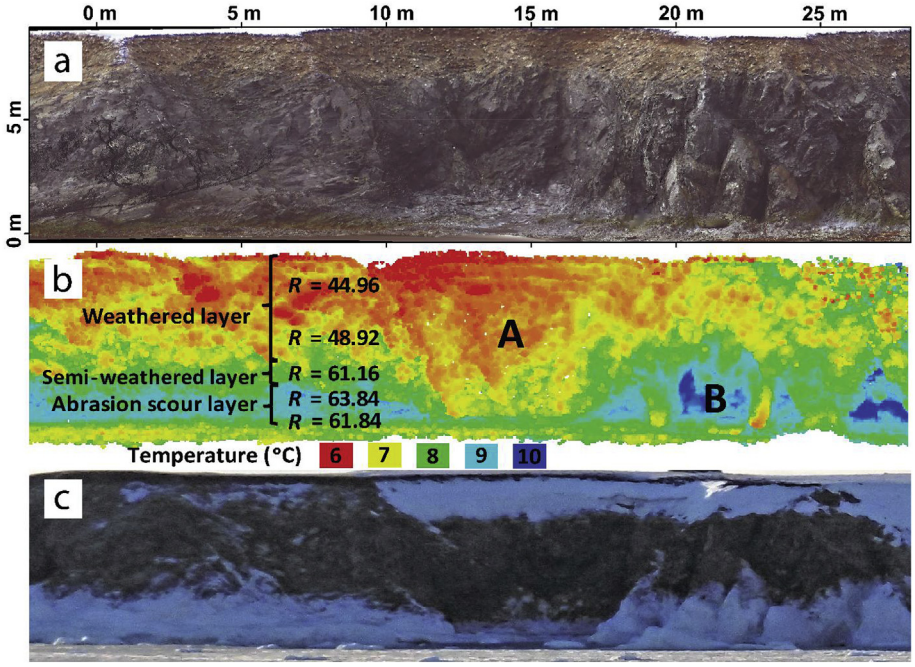

Fig. 5. Photogrammetric cliff surface model (a) and coincident three-dimensional temperature point cloud (b, coloured to reflect the inferred severity of weathering), with a vertical profile of Schmidt hammer readings (25 values averaged to a mean rebound value, R) over the accessible section of the monitored cliff. The lower image (c) is the site in March (2017) when the ice-foot transitions to decay; there appears to be a good spatial agreement with the thermal zones noted during the summer survey data.

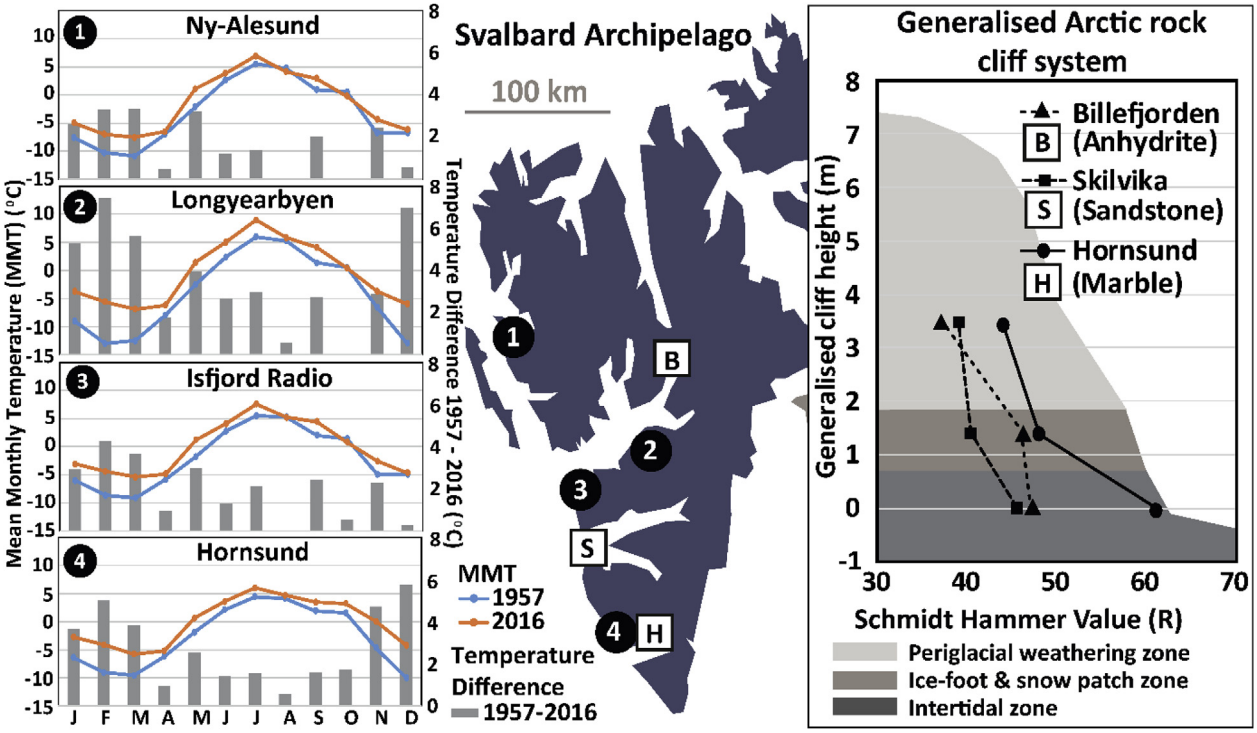

Fig. 6. Mean monthly temperatures (1957 and 2016) and the resultant differences at sites in a north-south transect through western Spitsbergen (left) and the averaged rock hardness values of key geomorphic process zones superimposed on a schematic diagram of rock coast morphology (right).

transition, decreasing with height up the cliff (Fig. 5). Here we suggest that the thermal and hardness differences reflect geomorphic process zones. Where the cliff base is impacted by dynamic ice contact from iceberg rafts, from ice-foot formation and movement, or from storm waves, the erosive agency is particularly effective. This agency is reflected by high rates of back wearing and by peak rock hardness (Blanco-Chao et al., 2007; Strzelecki et al., 2017). The ice-contact zone extends above the high water mark, and the scour and abrasive processes extend up to two thirds of the cliff height ('B' In Fig. 5b) on the most exposed spurs protruding out from the general line of the cliff face. In more sheltered areas such as embayments where ice movement potential is limited, this zone does not appear to exist and a weaker weathering zone dominates down to the cliff foot ('A' In Fig. 5b). The hardness values in these areas were up to a third lower than those recorded at the scoured cliff base. There is a transition zone between the scour and weathered zones where intermediate hardness values have been recorded. Questions remain over the origin of this transition, potentially evidencing historic scour processes that no longer, or rarely, persist at these elevations (or indeed removed under high rates of isostatic uplift) or the influence of extreme storm events that occur at a

frequency of several years (Degard and Sollid, 1993). These process zones have been visualised for the first time using three-dimensional temperature mapping, although further work is required to fully explore the potential of this approach for geomorphic studies.

The rock coast environment at Hornsund has been subjected to some of the most dramatic temperature shifts in the Arctic over recent decades (Hinzman et al., 2005), and as such its wider significance is twofold. Firstly, it provides an opportunity to explore geomorphic behaviour under extreme shifts in process activity. Models of rock coast development and response have often been linked to sea-level (Trenhaile, 2010), significant wave height (Norman et al., 2013) and seasonality (Hansom et al., 2014) but quantitative links between process environment changes and rock cliff material responses have remained controversial and challenging (Naylor et al., 2010; Rosser et al., 2013). Secondly, the sustained temperature rise experienced at Hornsund may serve as an indicator of changes likely to impact other regions as climate trends continue. The relative difference in rock hardness across targeted elevations within rock coast profiles provides a potentially simple quantitative indicator of the presence or absence and significance of geomorphic zones at other sites (Strzelecki et al., 2017).

A regional north-south transect of data on temperature variations and rock hardness profiles has been compiled (Fig. 6). Average hardness profiles have been taken through rock cliffs from representative lithologies at each site, but for comparability and clarity lithologies of similar hardness values have been presented. The hardness recorded within specific rock coast zones at any particular site are influenced by the local competence of the cliff material, but by using the same approach, relative differences in intact rock hardness can be compared using the standardised rebound value (Hansen et al., 2013). The hardness values essentially provide a chronology of weathering exposure (Kellerer-Pirklbauer et al., 2008), assuming no armouring effects of precipitated solutes or biofilms that may artificially increase hardness, processes noted in arid extreme environments (Viles and Goudie, 2004).

The west coast of Spitsbergen has undergone variable levels of warming since 1957, with peak temperature increases occurring in the south (Hornsund) and central inner fjord areas (Longyearbyen). In such areas, the warming has been most pronounced in the winter season when ice foot development occurs, producing rock hardness transitions from a strong peak in the intertidal and sea-ice zone to rapidly declining through the depleted ice-foot and subaerially weathered zones. By contrast, areas that have undergone less severe temperature increases maintain the average rock hardness level upwards through the sea-ice and ice-foot zone. For example, the mean hardness rebound values (R) for both the scoured, fresh intertidal rock and the subaerially weathered zone higher up the cliff face are comparable for Billefjorden and Skilvika (differences of $R = 1$ and $R = 2$ respectively between the two sites in the intertidal and weathered zones), but there is a notable difference ($R = 6$) in the hardness of the ice-foot zone measurements (Fig. 6). Therefore, hardness profiles can effectively identify weathering process zones without the need to make inferences on the driving processes, which can be intrinsic or extrinsic and often lack significance in global scale comparisons (Prémaillon et al., 2018).

5. Implications

Arctic coastal rock cliff retreat is commonly thought to be amongst the most effective of all denudation environments (Prick, 2003). Cryogenic weathering and frost wedging in particular have been found to play a significant role in the behaviour and material failure of rock walls (Degard and Sollid, 1993; Matsuoka, 2008), but recent concerns have focussed on the climatically driven increases in the exposure of the coast (Sessford et al., 2015). Increases in the open water season and in the intensity of storms associated with rising temperature has been widely hypothesised to result in an increase in rates of erosion on Arctic coastlines (Hinzman et al., 2005; Wojtysiak et al., 2018). Whilst valid for highly erosive coastal systems such as ice rich permafrost cliffs (Jones et al., 2009), the response of rock coasts appears to be more complex.

Historic rates of rock cliff change are extremely sparse and although the detailed study conducted by Jahn (1961) suggests that rates of rock wall recession have declined over this period there is insufficient validation to make a reliable quantitative assessment. However, the qualitative information is just as revealing. In 1958 the ice-foot is recorded to have persisted almost throughout the summer season (Jahn, 1961). During the 2014–2017 surveys presented here, the ice-foot formed during early November and was fully developed by late January, but the key difference with 1958 conditions appears to be that the ice-foot was still building throughout April (based on historic temperatures) whereas it now degrades through April and is gone by late May. The thermal regime during ice-foot formation is critical to its longevity through the melt season and the incorporation of icebergs from glacier outlets may provide a key control in ice-foot morphology, resulting in rougher, more sporadic accumulations that reach higher up the shore and cliff face (Wiseman et al., 1981). The Hansbreen generates icebergs that reach the Veslebogen coastline following storm events that carry them out of the fjord. In 1957 the Hansbreen terminus reached the valley mouth and calving events were released directly into the open coast providing a significantly greater frequency of icebergs to the cliff base (Vieli et al., 2002). Therefore, the impact of warming over the intervening period is twofold, producing both a reduction in the ice-foot formation duration and intensity and a reduction in the supply of ice from retreating and increasingly disconnected glacier systems.

There is no indication that temperature shifts in the Arctic, which have been particularly pronounced on the west coast of Spitsbergen, have transitioned from ice foot formation under storm and drift driven processes to tidal freezing processes that exert much more regular and height-constrained influence up the shoreface (Wiseman et al., 1981). There is potential to explore these system level responses through quantitative monitoring of rock hardness, perhaps through the ice free season and over successive seasons, particularly when combined with remotely sensed relative indicators of coastal process zones such as the three-dimensional thermal mapping presented here. The results from the historical study comparison suggest that the decline and ultimate loss of ice-foot processes (largely mechanical such as plucking and abrasive scour) from Arctic rock cliffs may currently be a more significant factor than the increased exposure to higher energy storms; dominating the geomorphic response. Further to this, the increased intensity of Arctic storms in spring noted by Wojtysiak et al. (2018), may expedite the seasonal break-up and removal of the ice-foot, in the past it persisted year-long (Wiseman et al., 1981). It is increasingly acknowledged that the temperature driven changes to the open water season affecting Svalbard is producing complex and variable coastal erosion responses that require further investigation (Sessford et al., 2015).

The distinctiveness and effectiveness of coastal Arctic cliff processes has been found to set them apart from other Arctic rock cliff environments (Wangensteen et al., 2007). The fit of the size-frequency domains to power-law distributions holds significant potential in understanding the relation between driving processes and responding rates and mechanisms of change and in predicting future developments (Teixeira, 2006). The power law distributions break down at changes below $1 \times 10^{-3}\,m^3$ (and there are possible indications of divergence from this scaling in magnitudes up to $1 \times 10^{-2}\,m^3$), with lower than modelled numbers being detected. To complete a rigorous assessment of the data, subsections of close range photogrammetric monitoring indicate that the power law scaling may hold for finer scales but at a reduced rate of change. These data have implications for understanding the geomorphic significance of the small scale changes that are often ignored in rock slope studies and highlight the impact of thresholding approaches commonly used to isolate and quantify volumetric change in survey datasets. However, the representation of such small areas relative to the

wider behaviour of the rock wall remains open to question, particularly given the potential for spatially varied responses to the cryogenic, marine and subaerial processes in operation (Naylor et al., 2012; Strzelecki, 2017; Wangensteen et al., 2007).

Many Arctic coastal systems are experiencing altered thermal and hydrological regimes associated with transitions from glacial to deglacial conditions and permafrost to non-permafrost environments. The use of thermal mapping over landforms presented here appears to hold potential for detecting moisture and temperature related weathering zones and thus in characterising geomorphic responses that are not readily visible with colour imagery. It has particular utility in the detection of moisture related influences, critical to periglacial (Hall et al., 2002) and rock coast (Degard and Sollid, 1993) environments. The focus here has been on the relative differences in temperature to aid characterisation and classification, but the close (± 1 °C) agreement with point based checks and the supporting differences in rock hardness readings also highlight the potential quantitative value of the approach.

The ability to delineate zones of geomorphic response provides the basis to more focused and rigorous investigations of behaviour, refining and contextualising rate estimates spatially and helping to inform rock coast models (Naylor et al., 2012). Questions raised from this research concern the origin and future evolution of these zones. In particular, whether the transitionary semi-weathered zone identified above the scoured base corresponds with storm waves and may increase in prominence with higher intensity events or represents an inherited feature from previous decades when the ice-foot extent remained higher for longer and will consequently decline in significance. The influence of ice on coastal geomorphology has the potential to both enhance erosion through scour, plucking and abrasion (Are et al., 2008; Dionne and Brodeur, 1988) and to mitigate it through thermal insulation (Scrosati and Eckersley, 2007) and by attenuating, dissipating and removing wave and tidal influence from the cliff face (Taylor and McCann, 1976). The spatial and temporal variability of ice-foot processes has long been recognised (Wiseman et al., 1981), complicating the interpretation and analysis of climatic influences on Arctic rock coast geomorphic behaviour. However, the indications of abrasive geomorphic zones that extend significantly beyond storm wave height suggest that cryogenic control may be a dominant but declining influence on these systems. These understudied aspects of Arctic coast landforms, often typified by either very low (André, 1997) or very high (Overduin et al., 2014) rates and intensities of weathering, erosion and denudation processes, have important implications for primary ecosystem development and nutrient availability (Borin et al., 2010) and for asset management of coastal infrastructure (Ford et al., 2010; Jaskólski et al., 2018).

6. Conclusion

The Arctic is undergoing system-wide responses to climate-induced change (Hinzman et al., 2005), affording a rare opportunity to assess rock coast responses in the context of process conditions that are altering over relatively recent (< 100 year) timescales. Utilising high resolution survey approaches, novel temperature mapping and monitoring and simple geotechnical characterisation we draw the following conclusions:

- Despite a reduction in sea-ice and greater storm intensity recorded in the Arctic rates of rock coast erosion are lower than those reported at the same site in 1961 (Jahn, 1961).
- Marked increases in temperatures during the winter months critical to ice-foot formation have resulted in significant decreases to the extent and duration of the ice-foot.
- Power law relationships effectively model Arctic rock cliff behaviour over several orders of magnitude, but an inflection demonstrated through lower exponents was detected in the scaling of low magnitude (below 1×10^{-6} m^3) rock falls.
- Temperature monitoring with depth into the shore platform, cliff face and cliff top has revealed the sensitivity of Arctic rock coasts to both global teleconnection events such as severe depressions and local influences such as ice-foot dynamics and the presence of icebergs.
- The application of three-dimensional thermal mapping to spatially map process zones, validated through quantitative rock hardness measurements, suggests a declining cryogenic influence in the most temperature affected areas of Spitsbergen.

Declaration of competing interest

The authors declare that they have no known competing financial interests or personal relationships that could have appeared to influence the work reported in this paper.

Acknowledgements

The authors thank and acknowledge the National Science Centre, Poland, for funding 'POROCO – Mechanisms controlling the evolution and geomorphology of rock coasts in polar climates' (UMO2013/11/B/ST10/00283). M.C.S contributed to the paper during the NAWA Bekker Programme Fellow (PPN/BEK/2018/1/00306) at Alfred Wegener Institute in Potsdam. The authors thank the staff of Polish Polar Station in Hornsund, Svalbard, for support in field logistics. We gratefully acknowledge the insightful and helpful reviews of Alan Trenhaile, an anonymous reviewer and the editorial team whose comments have been used to improve the paper.

References

André, M.-F., 1997. Holocene rockwall retreat in svalbard: a triple-rate evolution. Earth Surf. Process. Landforms 22, 423–440.
Are, F., Reimnitz, E., Grigoriev, M., Hubberten, H.W., Rachold, V., 2008. The influence of cryogenic processes on the erosional arctic shoreface. J. Coast. Res. 24, 110–121.
Barlow, J., Lim, M., Rosser, N., Petley, D., Brain, M., Norman, E., Geer, M., 2012. Modeling cliff erosion using negative power law scaling of rockfalls. Geomorphology 139, 416–424.
Berthling, I., Etzelmuller, B., 2011. The concept of cryo-conditioning in landscape evolution. Quat. Res. 75, 378–384.
Blanco-Chao, R., Pérez-Alberti, A., Trenhaile, A.S., Costa-Casais, M., Valcárcel-Díaz, M., 2007. Shore platform abrasion in a para-periglacial environment, Galicia, northwestern Spain. Geomorphology 83, 136–151.
Borin, S., Ventura, S., Tambone, F., Mapelli, F., Schubotz, F., Brusetti, L., Scaglia, B., D'Acqui, L.P., Solheim, B., Turicchia, S., Marasco, R., Hinrichs, K.-U., Baldi, F., Adani, F., Daffonchio, D., 2010. Rock weathering creates oases of life in a High Arctic desert. Environ. Microbiol. 12, 293–303.
Budetta, P., Galietta, G., Santo, A., 2000. A Methodology for the Study of the Relation between Coastal Cliff Erosion and the Mechanical Strength of Soils and Rock Masses.
Byrne, M.-L., Dionne, J.-C., 2002. Typical aspects of cold regions shorelines. In: Hewitt, K. (Ed.), Landscapes of Transition. Kluwer Academic, Dordrecht, pp. 141–158.
Collins, B.D., Stock, G.M., 2016. Rockfall triggering by cyclic thermal stressing of exfoliation fractures. Nat. Geosci. 9, 395.
Coombes, M.A., 2011. Rock warming and drying under simulated intertidal conditions, part I: experimental procedures and comparisons with field data. Earth Surf. Process. Landforms 36, 2114–2121.
Coombes, M.A., Viles, H.A., Naylor, L.A., La Marca, E.C., 2017. Cool barnacles: do common biogenic structures enhance or retard rates of deterioration of intertidal rocks and concrete? Sci. Total Environ. 580, 1034–1045.
Cullen, N.D., Verma, A.K., Bourke, M.C., 2018. A comparison of structure from motion photogrammetry and the traversing micro-erosion meter for measuring erosion on shore platforms. Earth Surf. Dyn. 6, 1023–1039.
Degard, R.S., Sollid, J.L., 1993. Coastal cliff temperatures related to the potential for cryogenic weathering processes, western Spitsbergen, Svalbard. Polar Res. 12, 95–106.
Dionne, J.-C., Brodeur, D., 1988. Frost weathering and ice action in shore platform development, with particular reference to Quebec, Canada. Z. Geomorphol. Supplement Band 71, 117–130.
Edis, E., Flores-Colen, I., de Brito, J., 2014. Passive thermographic detection of moisture problems in façades with adhered ceramic cladding. Constr. Build. Mater. 51, 187–197.
Eppes, M.-C., Keanini, R., 2017. Mechanical weathering and rock erosion by climate-dependent subcritical cracking. Rev. Geophys. 55, 470–508.
Etzelmüller, B., Schuler, T., Isaksen, K., Christiansen, H., Farbrot, H., Benestad, R., 2011. Modeling the Temperature Evolution of Svalbard Permafrost during the 20th and 21st Century.
Feagin, R.A., Williams, A.M., Popescu, S., Stukey, J., Washington-Allen, R.A., 2014. The

use of terrestrial laser scanning (TLS) in dune ecosystems: the lessons learned. J. Coast. Res. 30, 111–119.
Forbes, D.L., 2011. State of the arctic coast 2010 – scientific review and outlook. In: Helmholtz-Zentrum. International Permafrost Association, Geesthacht, Germany, pp. 178.
Forbes, D.L., Taylor, R.B., 1994. Ice in the shore zone and the geomorphology of cold coasts. Prog. Phys. Geogr. 18, 59–96.
Ford, J.D., Bell, T., St-Hilaire-Gravel, D., 2010. Vulnerability of community infrastructure to climate change in nunavut: a case study from arctic bay. In: Hovelsrud, G.K., Smit, B. (Eds.), Community Adaptation and Vulnerability in Arctic Regions. Springer Netherlands, Dordrecht, pp. 107–130.
Gilham, J., Barlow, J., Moore, R., 2018. Marine control over negative power law scaling of mass wasting events in chalk sea cliffs with implications for future recession under the UKCP09 medium emission scenario. Earth Surf. Process. Landforms 43, 2136–2146.
Gjelten, H.M., Nordli, O., Isaksen, K., Forland, E.J., Sviashchennikov, P.N., Wyszynski, P., Prokhorova, U.V., Przybylak, R., Ivanov, B.V., Urazgildeeva, A.V., 2016. Air temperature variations and gradients along the coast and fjords of western Spitsbergen. Polar Res. *35*.
Grinzato, E., Vavilov, V., Kauppinen, T., 1998. Quantitative infrared thermography in buildings. Energy Build. 29, 1–9.
Guerin, A., Hantz, D., Rossetti, J.P., Jaboyedoff, M., 2014. Brief communication"Estimating rockfall frequency in a mountain limestone cliff using terrestrial laser scanner. Nat. Hazards Earth Syst. Sci. Discuss 123–135 2014.
Hall, K., 1988. A laboatory simulation of rock breakdown due to freeze thaw in a maritime Antarctic environment. Earth Surf. Process. Landforms 13, 369–382.
Hall, K., Thorn, C.E., Matsuoka, N., Prick, A., 2002. Weathering in cold regions: some thoughts and perspectives. Prog. Phys. Geogr. 26, 577–603.
Hansen, C.D., Meiklejohn, K.I., Nel, W., Loubser, M.J., Van der merwe, B.J., 2013. Aspect-controlled weathering observed on a blockfield in dronning maud land, Antarctica. Geogr. Ann. Ser. A Phys. Geogr. 95, 305–313.
Hansom, J.D., Forbes, D.L., Etienne, S., 2014. The rock coasts of polar and sub-polar regions. In: K.D.M. (Ed.), Rock Coast Geomorphology: A Global Synthesis. Geological Society, London, Memoirs, pp. 263–504.
Herman, A., Wojtysiak, K., Moskalik, M., 2019. Wind wave variability in Hornsund fjord, west Spitsbergen. Estuar. Coast Shelf Sci. 217, 96–109.
Hinzman, L.D., Bettez, N.D., Bolton, W.R., Chapin, F.S., Dyurgerov, M.B., Fastie, C.L., Griffith, B., Hollister, R.D., Hope, A., Huntington, H.P., Jensen, A.M., Jia, G.J., Jorgenson, T., Kane, D.L., Klein, D.R., Kofinas, G., Lynch, A.H., Lloyd, A.H., McGuire, A.D., Nelson, F.E., Oechel, W.C., Osterkamp, T.E., Racine, C.H., Romanovsky, V.E., Stone, R.S., Stow, D.A., Sturm, M., Tweedie, C.E., Vourlitis, G.L., Walker, M.D., Walker, D.A., Webber, P.J., Welker, J.M., Winker, K., Yoshikawa, K., 2005. Evidence and implications of recent climate change in northern Alaska and other arctic regions. Clim. Change 72, 251–298.
Inkpen, R.J., Stephenson, W.J., Kirk, R.M., Hemmingsen, M.A., Hemmingsen, S.A., 2010. Analysis of relationships between micro-topography and short- and long-term erosion rates on shore platforms at Kaikoura Peninsula, South Island, New Zealand. Geomorphology 121, 266–273.
Jahn, A., 1961. Quantitative Analysis of Some Periglacial Processes in Spitsbergen. ([Warszawa]: [Panstwowe Wydawn. Naukowe]).
Jakacki, J., Przyborska, A., Kosecki, S., Sundfjord, A., Albretsen, J., 2017. Modelling of the svalbard fjord Hornsund. Oceanologia 59, 473–495.
Jaskólski, M., Pawłowski, Ł., Strzelecki, M., 2018. High Arctic coasts at risk-the case study of coastal zone development and degradation associated with climate changes and multidirectional human impacts in Longyearbyen (Adventfjorden, Svalbard). Land Degrad. Dev.
Jones, B.M., Arp, C.D., Jorgenson, M.T., Hinkel, K.M., Schmutz, J.A., Flint, P.L., 2009. Increase in the rate and uniformity of coastline erosion in Arctic Alaska. Geophys. Res. Lett. *36*.
Kellerer-Pirklbauer, A., Wangensteen, B., Farbrot, H., Etzelmuller, B., 2008. Relative surface age-dating of rock glacier systems near Holar in Hjaltadalur, northern Iceland. J. Quat. Sci. 23, 137–151.
Kim, B.M., Hong, J.Y., Jun, S.Y., Zhang, X.D., Kwon, H., Kim, S.J., Kim, J.H., Kim, S.W., Kim, H.K., 2017. Major cause of unprecedented Arctic warming in January 2016: critical role of an Atlantic windstorm. Sci. Rep. *7*.
Kirk, R.M., 1977. Rates and forms of erosion on intertidal platforms at kaikoura peninsula, south island, New Zealand. N. Z. J. Geol. Geophys. 20, 571–613.
Krautblatter, M., Moser, M., Schrott, L., Wolf, J., Morche, D., 2012. Significance of rockfall magnitude and carbonate dissolution for rock slope erosion and geomorphic work on Alpine limestone cliffs (Reintal, German Alps). Geomorphology 167–168, 21–34.
Lantuit, H., Overduin, P.P., Couture, N., Wetterich, S., Are, F., Atkinson, D., Brown, J., Cherkashov, G., Drozdov, D., Forbes, D.L., Graves-Gaylord, A., Grigoriev, M., Hubberten, H.W., Jordan, J., Jorgenson, T., Odegard, R.S., Ogorodov, S., Pollard, W.H., Rachold, V., Sedenko, S., Solomon, S., Steenhuisen, F., Streletskaya, I., Vasiliev, A., 2012. The arctic coastal dynamics database: a new classification scheme and statistics on arctic permafrost coastlines. Estuar. Coasts 35, 383–400.
Lim, M., Petley, D.N., Rosser, N.J., Allison, R.J., Long, A.J., Pybus, D., 2005. Combined digital photogrammetry and time-of-flight laser scanning for monitoring cliff evolution. Photogramm. Rec. 20 109-+.
Lim, M., Rosser, N.J., Allison, R.J., Petley, D.N., 2010. Erosional processes in the hard rock coastal cliffs at Staithes, North Yorkshire. Geomorphology 114, 12–21.
Lim, M., Rosser, N.J., Petley, D.N., Keen, M., 2011. Quantifying the controls and influence of tide and wave impacts on coastal rock cliff erosion. J. Coast. Res. 27, 46–56.
Limber, P.W., Murray, A.B., 2011. Beach and sea-cliff dynamics as a driver of long-term rocky coastline evolution and stability. Geology 39, 1147–1150.
Luscombe, D.J., Anderson, K., Gatis, N., Grand-Clement, E., Brazier, R.E., 2015. Using airborne thermal imaging data to measure near-surface hydrology in upland ecosystems. Hydrol. Process. 29, 1656–1668.
Matsuoka, N., 2008. Frost weathering and rockwall erosion in the southeastern Swiss Alps: long-term (1994–2006) observations. Geomorphology 99, 353–368.
Matsuoka, N., Moriwaki, K., Hirakawa, K., 1996. Field experiments on physical weathering and wind erosion in an Antarctic cold desert. Earth Surf. Process. Landforms 21, 687–699.
Naylor, L.A., Stephenson, W.J., Trenhaile, A.S., 2010. Rock coast geomorphology: recent advances and future research directions. Geomorphology 114, 3–11.
Naylor, L.A., Coombes, M.A., Viles, H.A., 2012. Reconceptualising the role of organisms in the erosion of rock coasts: a new model. Geomorphology 157–158, 17–30.
Naylor, L.A., Spencer, T., Lane, S.N., Darby, S.E., Magilligan, F.J., Macklin, M.G., Möller, I., 2017. Stormy geomorphology: geomorphic contributions in an age of climate extremes. Earth Surf. Process. Landforms 42, 166–190.
Nielsen, N., 1979. Ice-foot processes. Observations of erosion of the rocky coast, Disko, West Greenland. Z. Geomorphol. 23, 321–331.
Norman, E.C., Rosser, N.J., Brain, M.J., Petley, D.N., Lim, M., 2013. Coastal cliff-top ground motions as proxies for environmental processes. J. Geophys. Res. Oceans 118, 6807–6823.
Overduin, P.P., Strzelecki, M.C., Grigoriev, M.N., Couture, N., Lantuit, H., St-Hilaire-Gravel, D., Günther, F., Wetterich, S., 2014. Coastal changes in the arctic. In: Martini, I.P. (Ed.), Sedimentary Coastal Zones from High to Low Latitudes: Similarities and Differences. Geological Society. In: Wanless, H.R. (Ed.), vol. 388. Special Publications, London, pp. 103–129.
Overeem, I., Anderson, R.S., Wobus, C.W., Clow, G.D., Urban, F.E., Matell, N., 2011. Sea ice loss enhances wave action at the Arctic coast. Geophys. Res. Lett. 38.
Parkinson, C.L., Comiso, J.C., 2013. On the 2012 record low Arctic sea ice cover: combined impact of preconditioning and an August storm. Geophys. Res. Lett. 40, 1356–1361.
Prémaillon, M., Regard, V., Dewez, T.J.B., Auda, Y., 2018. GlobR2C2 (Global Recession Rates of Coastal Cliffs): a global relational database to investigate coastal rocky cliff erosion rate variations. Earth Surf. Dyn. 6, 651–668.
Prick, A., 2002. Monitoring weathering and erosion of bedrock on a coastal cliff, Longyearbyen, Svalbard. In: Rachold, V.B., J., Solomon, S., Sollid, J.L. (Eds.), Arctic Coastal Dynamics: Report of the 3rd International Workshop University of Oslo (Norway) 2-5 December 2002, (pp. 95–95). Oslo, Norway: Reports on Polar and Marine Research.
Prick, A., 2003. Frost weathering and rock fall in an Arctic Environment, Longyerbyen, Svalbard. In: Phillips, M., Springman, S.M., Arenson, L.U. (Eds.), Permafrost, Proceedings of the Eight International Conference on Permafrost, 21-25 July, Zürich, Switzerland. 2. Balkema, Lisse, pp. 907–912.
Rapp, A., 1957. Studien über Schutthalden in Lappland und auf Spitzbergen. Z. Geomorphol. 1, 179–200.
Rasmussen, T.L., Thomsen, E., Slubowska, M.A., Jessen, S., Solheim, A., Koc, N., 2007. Paleoceanographic evolution of the SW Svalbard margin (76 degrees N) since 20,000 C-14 yr BP. Quat. Res. 67, 100–114.
Rohmer, J., Dewez, T., 2015. Analysing the spatial patterns of erosion scars using point process theory at the coastal chalk cliff of Mesnil-Val, Normandy, northern France. Nat. Hazards Earth Syst. Sci. 15, 349–362.
Rosser, N., Lim, M., Petley, D., Dunning, S., Allison, R., 2007. Patterns of precursory rockfall prior to slope failure. J. Geophys. Res. Earth Surf. *112*.
Rosser, N.J., Brain, M.J., Petley, D.N., Lim, M., Norman, E.C., 2013. Coastline retreat via progressive failure of rocky coastal cliffs. Geology 41, 939–942.
Sass, O., 2005. Rock moisture measurements: techniques, results, and implications for weathering. Earth Surf. Process. Landforms 30, 359–374.
Scrosati, R., Eckersley, L.K., 2007. Thermal insulation of the intertidal zone by the ice foot. J. Sea Res. 58, 331–334.
Sessford, E.G., Baeverford, M.G., Hormes, A., 2015. Terrestrial processes affecting unlithified coastal erosion disparities in central fjords of Svalbard. Polar Res. *34*.
Stemberk, J., Briestenský, M., Cacoń, S., 2015. The recognition of transient compressional fault slow – slip along the northern shore of Hornsund Fjord, SW Spitsbergen, Svalbard. Pol. Polar Res. 36, 109–123.
Stephenson, W.J., Finlayson, B.L., 2009. Measuring erosion with the micro-erosion meter—contributions to understanding landform evolution. Earth Sci. Rev. 95, 53–62.
Stephenson, W.J., Kirk, R.M., 2001. Surface swelling of coastal bedrock on inter-tidal shore platforms, Kaikoura Peninsula, South Island, New Zealand. Geomorphology 41, 5–21.
Strzelecki, M.C., 2011. Schmidt hammer tests across a recently deglacierized rocky coastal zone in Spitsbergen - is there a "coastal amplification" of rock weathering in polar climates? Pol. Polar Res. 32, 239–252.
Strzelecki, M.C., 2017. The variability and controls of rock strength along rocky coasts of central Spitsbergen, High Arctic. Geomorphology 293, 321–330.
Strzelecki, M.C., Kasprzak, M., Lim, M., Swirad, Z.M., Jaskólski, M., Pawłowski, Ł., Modzel, P., 2017. Cryo-conditioned rocky coast systems: a case study from Wilczekodden, Svalbard. Sci. Total Environ. 607–608, 443–453.
Sunamura, T., 1992. Geomorphology of Rocky Coasts. pp. 302.
Swirad, Z.M., Migoń, P., Strzelecki, M.C., 2017. Rock control on the shape of coastal embayments of north-western Hornsund, Svalbard. Z. Geomorphol. 61, 11–28.
Taylor, R.B., McCann, B., 1976. The effect of sea and nearshore ice on coastal processes. Rev. Geogr. Montreal 30, 123–132.
Teixeira, S., 2006. Slope Mass Movements on Rocky Sea-Cliffs: A Power-Law Distributed Natural Hazard on the Barlavento Coast. (Algarve, Portugal).
Trenhaile, A.S., 1983. The Development of Shore Platforms in High Latitudes. In: Smith, D.E., Dawson, A.G. (Eds.), Shorelines and Isostasy. Institute of British Geographers, London, pp. 77–96.

Trenhaile, A.S., 1997. Coastal Dynamics and Landforms. Oxford University Press, Oxford.
Trenhaile, A.S., 2010. The effect of Holocene changes in relative sea level on the morphology of rocky coasts. Geomorphology 114, 30–41.
van Veen, M., Hutchinson, D.J., Kromer, R., Lato, M., Edwards, T., 2017. Effects of sampling interval on the frequency-magnitude relationship of rockfalls detected from terrestrial laser scanning using semi-automated methods. Landslides 14, 1579–1592.
Vieli, A., Jania, J., Kolondra, L., 2002. The retreat of a tidewater glacier: observations and model calculations on Hansbreen, Spitsbergen. J. Glaciol. 48, 592–600.
Viles, H.A., Goudie, A.S., 2004. Biofilms and case hardening on sandstones from Al-Quwayra, Jordan. Earth Surf. Process. Landforms 29, 1473–1485.
Wangensteen, B., Eiken, T., Odegard, R.S., Sollid, J.L., 2007. Measuring coastal cliff retreat in the Kongsfjorden area, Svalbard, using terrestrial photogrammetry. Polar Res. 26, 14–21.
Webster, C., Westoby, M., Rutter, N., Jonas, T., 2018. Three-dimensional thermal characterization of forest canopies using UAV photogrammetry. Remote Sens. Environ. 209, 835–847.
Westoby, M.J., Lim, M., Hogg, M., Pound, M.J., Dunlop, L., Woodward, J., 2018. Cost-effective erosion monitoring of coastal cliffs. Coast. Eng. 138, 152–164.
Wiseman, W.J., Owens, E.H., Kahn, J., 1981. Temporal and spatial variability of ice-foot morphology. Geogr. Ann. Ser. A Phys. Geogr. 63, 69–80.
Wojtysiak, K., Herman, A., Moskalik, M., 2018. Wind wave climate of west Spitsbergen: seasonal variability and extreme events. Oceanologia 60, 331–343.
Young, A.P., Olsen, M.J., Driscoll, N., Flick, R.E., Gutierrez, R., Guza, R.T., Johnstone, E., Kuester, F., 2010. Comparison of airborne and terrestrial lidar estimates of seacliff erosion in southern California. Photogramm. Eng. Remote Sens. 76, 421–427.